Pre-Steady-State Kinetics of Nucleotide Insertion following 8-Oxo-7,8-dihydroguanine Base Pair Mismatches by Bacteriophage T7 DNA Polymerase exo^{-}[†]

Laura Lowe Furge[‡] and F. Peter Guengerich*

Department of Biochemistry and Center in Molecular Toxicology, Vanderbilt University School of Medicine, Nashville, Tennessee 37232-0146

Received September 8, 1997; Revised Manuscript Received January 9, 1998

ABSTRACT: 8-Oxo-7,8-dihydroguanine (8-oxoGua) can base pair with either cytosine (C) or adenine (A) when replicated by DNA polymerases. The 8-oxoGua·A mismatch is extended in preference to the 8-oxoGua·C pair. Using a model 25-mer/36-mer DNA duplex containing either guanine (Gua)·C, 8-oxoGua·C, or 8-oxoGua·A base pairs at the primer terminus and A at the standing start position, we found that the pre-steady-state addition of dTTP opposite A following all three base pairs by bacteriophage T7 DNA polymerase exo^{-} showed burst kinetics, suggesting that extension of all three base pairs is controlled by the rate of a step at or before phosphodiester bond formation. Substitution of dTTPαS for dTTP yielded modest thio effects of 1−6, suggesting that extension of all three pairs is limited by the rate of the conformational change prior to phosphodiester bond formation. Pre-steady-state values for k_{pol} (maximum polymerization rate) were 120, 12, and 28 s^{-1}, and K_d values were 2, 75, and 22 μM for insertion of dTTP following Gua·C, 8-oxoGua·C, and 8-oxoGua·A base pairs, respectively. Additional analysis of extension was provided by substitution of A in the standing start position by 2-aminopurine (2-AP), a fluorescent base analogue. Comparison of rapid-quench gel-based assays with stopped-flow fluorescence quenching assays suggested that during addition of dTTP opposite 2-AP phosphodiester bond formation was rate-limiting when 8-oxoGua·C or 8-oxoGua·A were the preceding base pairs, while conformational change was rate-limiting when Gua·C was the preceding base pair. Furthermore, the difference in apparent conformational change rates for addition of dTTP opposite 2-AP following the 8-oxoGua base pairs was greater than the differences in their phosphodiester bond formation rates, suggesting that discrimination in extension may be influenced more by conformational change rates than the rates of phosphodiester bond formation in this mispaired system.

DNA adducts are formed by the covalent interaction of reactive chemical species with DNA. Mutations and base pair substitutions occurring during replication of DNA adducts by DNA polymerases result from the capacity of DNA adducts to base pair with noncomplementary bases in addition to or rather than complementary bases. The role of DNA polymerases in correct replication of DNA adducts depends partly on the efficiency of the polymerase to select the correct base for insertion opposite the adduct, which in turn depends on the sequence context of the adduct and mispair, the type of adduct and mispair formed, and the specific polymerase responsible for the replication. Following a misinsertion, the polymerase may dissociate from the DNA, excise the mispair if the polymerase has exonuclease activity, or extend the mispair to seal the mutation. In normal mispairs, i.e., non-Watson−Crick base pairs not involving DNA adducts, the rate of extension of the mispair is slower than the rate of base excision, allowing the polymerase time to correct the misinsertion (*1, 2*). Also, it is likely that phosphodiester bond formation is the rate-limiting step in the mechanism of normal mispair extension (*3*). Thus, an additional "lesser known" mechanism for polymerase fidelity is provided by the kinetic barrier of slow extension of mismatches (*4*−*8*).

When a DNA adduct is involved in a mispair, there are additional caveats to the extension kinetics that may help define a significant factor in the mutagenicity of DNA adducts. Contrary to the effect of slow extension of non-Watson−Crick base pairs, extension of many adduct mispairs is more efficient than extension of adduct "correct" pairs. Dosanjh et al. (*9*) showed that the "mutagenic" O^6-

[†] This work was supported in part by U.S. Public Health Service Grants R35 CA44353 and P30 ES00267. L.L.F. was supported in part by USPHS Training Grant T32 ES07028.

* To whom correspondence should be addressed at the Department of Biochemistry, Vanderbilt University School of Medicine, Nashville, TN 37232-0146. Telephone: (615) 322-2261. FAX: (615) 322-3141. E-mail: guengerich@toxicology.mc.vanderbilt.edu.

[‡] Formerly Laura G. Lowe

[1] Abbreviations: 8-oxoGua, 8-oxo-7,8-dihydroguanine; dNTPαS, α-thiodeoxynucleoside triphosphate; Gua, guanine; Ade or A, adenine; Cyt or C, cytidine; Thy or T, thymine; 2-AP, 2-aminopurine; EDTA, (ethylenedinitrilo)tetraacetic acid; T7, bacteriophage T7 DNA polymerase exo^{+}; T7^{-}, bacteriophage T7 DNA polymerase exo^{-}; HIV-1 RT, human immunodeficiency virus-1 reverse transcriptase; KF^{+}, *Escherichia coli* polymerase I (Klenow fragment) exo^{+}; KF^{-}, *E. coli* pol I (Klenow fragment) exo^{-}; pol II^{-}, *E. coli* polymerase II exo^{-}; Tris, tris(hydroxymethyl)aminomethane; DTT, dithiothreitol.

S0006-2960(97)02209-5 CCC: $15.00
Published on Web 02/20/1998

methylGua·T[1] base pair was efficiently extended while the "correct" pair O^6-methylGua·C was a block to replication. The same was true for the mutagenic pairs O^4-ethylThy·G and O^4-methylThy·G and the "correct" pairs O^4-ethylThy·A and O^4-methylThy·A; the later two were replication blocking while the former were efficiently extended (*10*). The bulky lesion *trans*-(+)-*anti*-benzo[*a*]pyrenediol epoxide-N^2-Gua was also extended more efficiently when it was paired with A rather than the correct base C (*11*). The 1,N^2-propanoGua·A mutagenic pair was efficiently extended to full-length product while the "correct" pair 1,N^2-propanoGua·C was extended only after slippage of the template (*12*). Furthermore, the major factor contributing to the presence of A opposite 1,N^2-propanoGua in full-length product was preferential extension of the 1,N^2-propanoGua·A mispair to full-length (*12*). Thus, in contrast to the situation encountered with mismatches of the four normal bases, a general phenomenon of preferential extension of the adduct mispair has been defined in the literature, although the initial misinsertion event may not be favored over correct nucleotide insertion.

The most abundant DNA adduct formed from reactive oxygen species is 8-oxoGua. Due to its ability to base pair with both C and A, 8-oxoGua causes G to T transversions when replicated by DNA polymerases. Preferential extension of the 8-oxoG·A mispair over the 8-oxoG·C "correct" pair was first reported in the literature by Shibutani et al. (*13*). We subsequently found in pre-steady-state rapid-quench assays with KF$^-$, pol II$^-$, HIV-1 RT, and T7$^-$ that the rate of extension of the 8-oxoGua·A mispair was greater than that of the 8-oxoG·C pair (*14*, *15*). In the cases of KF$^-$, pol II$^-$, and HIV-1 RT, the biphasic kinetics observed during extension of 8-oxoG·A were absent during extension of 8-oxoG·C. However, with T7$^-$, extension of both pairs showed biphasic kinetics with the burst rate for extension of 8-oxoG·C being slower than that for extension of 8-oxoG·A (*15*). This result provided the opportunity for detailed exploration of the mechanistic bases for the preferential extension of the 8-oxoG·A pair. Specifically, by using rapid-quench and stopped-flow fluorescence quenching assays, we have addressed the questions of what the kinetic barriers are to extension of adduct-containing base pairs and why the adduct mispair is preferentially extended over the "correct" pair.

EXPERIMENTAL PROCEDURES

T7$^-$ and Thioredoxin. The overproducing strains for T7$^-$ and thioredoxin were provided by Prof. K. A. Johnson (Pennsylvania State University). The proteins were purified to electrophoretic homogeneity (*16*) as described by Patel et al. (*17*) and Lunn et al. (*18*). Protein concentrations were estimated using $\epsilon_{280} = 144$ mM^{-1} cm^{-1} for T7$^-$ and $\epsilon_{280} = 13.7$ mM^{-1} cm^{-1} for thioredoxin. Purified T7$^-$ was stored in small aliquots at −70 °C in 20 mM potassium phosphate buffer (pH 7.4) containing 0.1 mM EDTA, 1.0 mM DTT, and 50% glycerol (v/v). Thioredoxin was also stored in small aliquots at −70 °C in 50 mM Tris-HCl buffer (pH 8.5) containing 3 mM EDTA and 50% glycerol (v/v). T7$^-$ was reconstituted with thioredoxin immediately prior to use as described (*15*, *17*). The activity of T7$^-$ was determined to be nearly 100% in active-site titration experiments described previously (*15*).

Table 1: Oligonucleotides[a]

36G-mer template with	5′-GCC TCG AGC CAG CCG CAG ACG CAG A
25C-mer and 25A-mer	5′-GCC TCG AGC CAG CCG CAG ACG CAG C
	3′-CGG AGC TCG GTC GGC GTC TGC GTC GAT CCT GCG GCT
36-8-oxoG-mer template with	5′-GCC TCG AGC CAG CCG CAG ACG CAG A
25C-mer and 25A-mer	5′-GCC TCG AGC CAG CCG CAG ACG CAG C
	3′-CGG AGC TCG GTC GGC GTC TGC GTC **G**AT CCT GCG GCT
36G-mer template with 2-AP	5′-GCC TCG AGC CAG CCG CAG ACG CAG A
and 25C-mer and 25A-mer	5′-GCC TCG AGC CAG CCG CAG ACG CAG C
	3′-CGG AGC TCG GTC GGC GTC TGC GTC G **2-AP** T CCT GCG GCT
36-8-oxoG-mer template with 2-AP	5′-GCC TCG AGC CAG CCG CAG ACG CAG A
and 25C-mer and 25A-mer	5′-GCC TCG AGC CAG CCG CAG ACG CAG C
	3′-CGG AGC TCG GTC GGC GTC TGC GTC **G 2-AP** T CCT GCG GCT

[a] **G** denotes the position of 8-oxoGua.

Nucleoside Triphosphates. Unlabeled Ultrapure Grade dNTPs were purchased from Pharmacia Biotech (Uppsala, Sweden), (S_p)-dNTPαSs were purchased from United States Biochemical Corp. (Cleveland, OH), and all radioisotopes were purchased from DuPont−New England Nuclear (Boston, MA).

Oligonucleotides. The oligonucleotide sequences chosen for these experiments are shown in Table 1. The sequences for primers (25-mer with 3′-A and 25-mer with 3′-C, designated 25A-mer and 25C-mer, respectively) were the same as those used previously in this lab (*15*), except that an A or 2-AP was placed 5′ of the standing start position, i.e., next to either the Gua control base or the 8-oxoGua base. The primers were purchased as "trityl-on" oligonucleotides from Midland Certified Reagent Co. (Midland, TX). All other oligonucleotides were synthesized as trityl-on oligonucleotides on an Expedite Nucleic Acid Synthesis System (Millipore Corp., Bedford, MA). The 8-oxoGua and 2-AP phosphoramidites were purchased from Glen Research (Sterling, VA). Oligonucleotides were detritylated and purified using NENSORB PREP cartridges (E. I. du Pont de Nemours & Co., Boston, MA), followed by purification by gel electrophoresis. The oligonucleotides were eluted from the gel as described (*14*) and recovered and concentrated with MICROPURE Inserts and MICRON Microconcentrators, respectively, from Amicon (Beverly, MA). The purity of all oligonucleotides was determined to be >99% by capillary gel electrophoresis using Beckman P/ACE 2000 and 5000 instruments (Beckman, Fullerton, CA) as described previously (*15*). Concentrations of purified oligonucleotides were estimated by UV absorbance (260 nm) from spectra determined using a modified Cary-14/OLIS spectrophotometer (On-Line Instrument Systems, Bogart, GA). Extinction coefficients were as follows: 25A-mer, $\epsilon_{260} = 237$ mM^{-1} cm^{-1}; 25C-mer, $\epsilon_{260} = 230$ mM^{-1} cm^{-1}; 36G-mer, $\epsilon_{260} = 319$ mM^{-1} cm^{-1}; 36-8-oxoG-mer, $\epsilon_{260} = 319$ mM^{-1} cm^{-1}; 36G-mer with 2-AP, $\epsilon_{260} = 319$ mM^{-1} cm^{-1}; and 36-8-oxoG-mer with 2-AP, $\epsilon_{260} = 319$ mM^{-1} cm^{-1} (*19*).

Primer End Labeling and Primer/Template Annealing. Primers were 5′-end-labeled using T4 polynucleotide kinase (Gibco BRL Life Technologies, Grand Island, NY) with [γ-^{32}P]ATP (3000 Ci/mmol) as previously described (*20*) and as modified in this laboratory (*14*).

Steady-State Incorporation of dTTP Opposite A following Gua·C, Gua·A, 8-OxoGua·C, or 8-OxoGua·A Base Pairs. The general approach of Boosalis et al. (*20*) was used, as modified in this laboratory (*14*, *15*). Steady-state reaction mixtures with T7$^-$ and the 25C-mer/36G-mer complex used

0.3 nM T7⁻, 100 nM duplex DNA, and 0.05−3.0 μM dTTP (final concentrations) and were run for 3.5 min. For steady-state assays with T7⁻ and the 25A-mer/36G-mer complex, 5.2 nM T7⁻, 100 nM duplex DNA, and 40−2000 μM dTTP were used in 10 min reactions. Steady-state reactions with T7⁻ and the 25C-mer/36-8-oxoG-mer complex used 0.7 nM T7⁻, 100 nM duplex DNA, and 1.0−40 μM dTTP and were run for 5 min. T7⁻ reactions with the 25A-mer/36-8-oxoG-mer complex also used 0.7 nM T7⁻ and 100 nM duplex DNA and were run for 5 min, but the concentration of dTTP varied from 0.1 to 1.5 μM. Reactions were initiated by the addition of an equal volume of dNTP in 100 mM Tris-HCl buffer (pH 7.4) containing 25 mM $MgCl_2$ (buffer A) (final concentrations of Tris-HCl and $MgCl_2$ were 50 and 12.5 mM, respectively) to preincubated enzyme/DNA solution. All reactions were quenched with twice the reaction volume of 20 mM EDTA at pH 7.4 (13 mM final concentration). All reactions were done in duplicate and at 25 °C. Products were analyzed by gel electrophoresis and quantitated as described previously (*14, 15*).

Pre-Steady-State Rapid-Quench Experiments. Rapid-quench experiments were carried out in a KinTek Quench-Flow Apparatus (Model RQF-3, KinTek Corp., State College, PA). Reactions were started by rapid mixing of ^{32}P-primer/template/polymerase mixtures (21.5 μL) with dTTP in buffer A (26.3 μL) and then quenched with an equal volume of 0.6 M EDTA, pH 7.4 (*17, 21*). The final concentration of duplex DNA in all reactions was 102 nM. The final concentration of T7⁻ varied as did dTTP concentrations (as reported in figure legends). Products were analyzed by gel electrophoresis and quantitated as described previously (*14, 15*). Pre-steady-state experiments, except where indicated, were fit with the burst equation: $y = A(1 - e^{-k_p t}) + k_{ss}t$, where A = burst amplitude, k_p = pre-steady-state rate constant for nucleotide incorporation,[2] t = time, and k_{ss} = steady-state rate of nucleotide incorporation. Graphs shown were generated in KaleidaGraph version 3.0.5. (Synergy Software, Reading, PA). KaleidaGraph software is equipped with nonlinear regression routines and error analysis which provide a best fit of the equations to the data (these equations are indicated in the figure legends and text).

Single-Turnover Elemental Effect for Incorporation following a Gua·A Base Pair. To evaluate a possible elemental effect during incorporation of dTTPαS opposite A following a Gua·A base pair, single-turnover analysis was used. Reactions with both dTTP and the thio analogue, dTTPαS, were done with final concentrations of 2, 4, 6, and 9 mM dNTP, 100 nM duplex DNA, and 70 nM T7⁻. Reactions were initiated by the manual mixing of equal volumes of ^{32}P-primer/template/enzyme mixture and dTTP or dTTPαS in buffer A followed by quenching with twice the reaction volume of 20 mM EDTA at pH 7.4 (13 mM final concentration). Reactions were done in duplicate and at 23 °C.

Pre-Steady-State Stopped-Flow Fluorescence Quenching Experiments. Fluorescence quenching assays were done using an Applied Photophysics SX-17MV stopped-flow spectrophotometer (Leatherhead, U.K.). An excitation wavelength of 310 nm was used in assays monitoring 2-AP fluorescence quenching. Emission was monitored by use of a 335-nm cutoff filter. Data were collected and analyzed using the software package and Acorn A5000 computer provided by Applied Photophysics. Reactions were initiated by rapid mixing of equal volumes of primer/template/polymerase mixtures with dTTP in buffer A. All reactions were at 25 °C. Traces are presented as averages of several individual reactions (4−10 reactions), and analysis of residuals provided by the manufacturer's software are shown below the plots.

RESULTS

Pre-Steady-State Kinetics of dTTP Incorporation Opposite A following Gua·C, 8-OxoGua·C, and 8-OxoGua·A Base Pairs. Pre-steady-state reactions were initiated by the rapid mixing of a preincubated solution of duplex DNA and T7⁻ (∼3-fold excess DNA) with dTTP in buffer A (Figure 1). Incorporation of dTTP opposite A following Gua·C, 8-oxoGua·C, and 8-oxoGua·A base pairs showed biphasic kinetics in all cases. The normal dTTP was replaced by the thio analogue, dTTPαS, for analysis of the elemental effect on the bursts (Figure 1). Relatively small thio effects of 1, 6, and 5 were observed for incorporation following Gua·C, 8-oxoGua·C, and 8-oxoGua·A base pairs, respectively (Figure 1).

Determination of K_d and k_{pol}. By varying the concentration of dTTP, the dependence of the burst phase rate on the concentration of dTTP was determined by single-exponential analysis as described previously (Figure 2 and other data not shown) (*14, 15*). The rate of the burst phase for each concentration of dTTP was then plotted against the respective concentration of dTTP and the hyperbola $k_{obs} = \{k_{pol}[dTTP]/([dTTP] + K_d)\}$ fit to the data, which describes the reaction equation:

$$E{\cdot}D + N \overset{K_d}{\rightleftharpoons} E{\cdot}D{\cdot}N \xrightarrow{k_{pol}} E{\cdot}D_{n+1}{\cdot}PP_i$$

where K_d = dNTP dissociation constant, k_{pol} = maximum rate for nucleotide incorporation, E = enzyme, D = 25/36-mer oligomer, N = dTTP, D_{n+1} = 26/36-mer product oligomer, and PP_i = pyrophosphate (Figure 2). The K_d^{dTTP} values for extension of Gua·C, 8-oxoGua·C, and 8-oxoGua·A base pairs were 2 ± 1 μM, 75 ± 37 μM, and 22 ± 4 μM, respectively (Figure 2). The k_{pol} values for extension of Gua·C, 8-oxoGua·C, and 8-oxoGua·A were 120 ± 9 s^{-1}, 12 ± 2 s^{-1}, and 28 ± 2 s^{-1} (Figure 2). The efficiency of extension (k_{pol}/K_d) was in the order Gua·C > 8-oxoGua·A > 8-oxoGua·C > Gua·A (Table 2). Steady-state efficiency of extension, k_{cat}/K_m (*9,22*), followed the same trend (Table 2).

Elemental Effect for dTTP Incorporation following Gua·A. To determine the rate-limiting step for incorporation of dTTP following the Gua·A mismatch, studies on the elemental effect were performed with 70 nM T7⁻, 100 nM duplex DNA, and 2, 4, 6, or 9 mM of either dTTP or dTTPαS (final concentrations) (Figure 3 and Supporting Information). The time course for addition of 2 mM dTTP yielded a rate of 6.7×10^{-3} s^{-1}. Upon substitution of 2 mM dTTP with 2 mM dTTPαS, the rate was reduced to 4.6×10^{-5} s^{-1}, yielding a thio effect of 150 (Figure 3). Similar thio effects of 130−165 were observed with near saturating dTTP and

[2] The parameter "k_p" is defined in the text as the pseudo-first-order rate constant while "k_{pol}" is defined in the text as the maximum rate for dNTP incorporation.

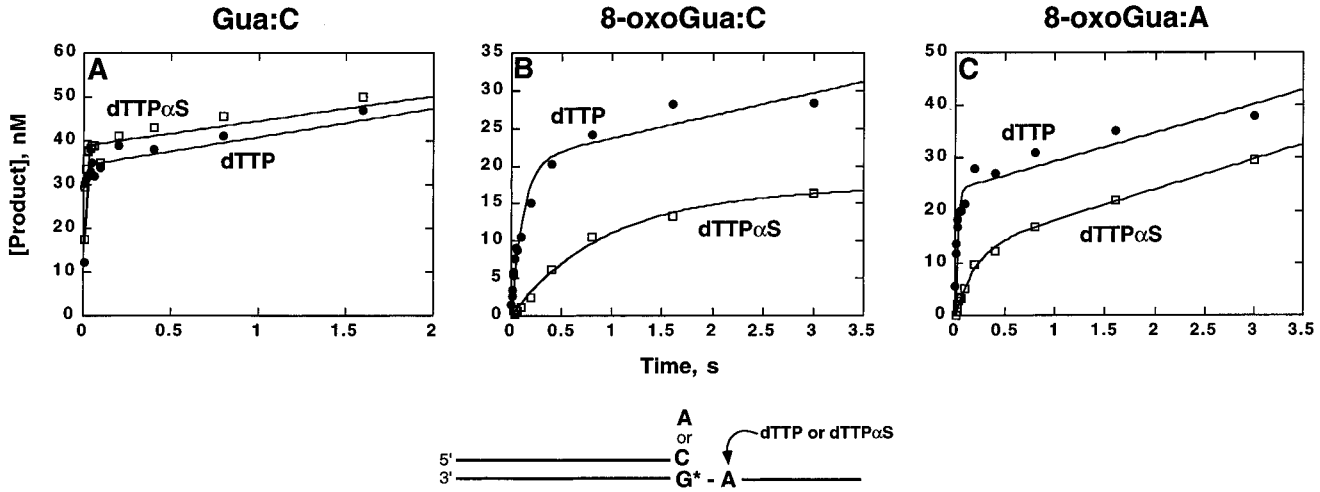

FIGURE 1: Time progress and elemental effect for dTTP addition opposite A following Gua·C, 8-oxoGua·C, and 8-oxoGua·A base pairs. (A) T7$^-$ (29 nM, preincubated with 102 nM 25C/36G-mer) was mixed with a solution of dTTP (220 μM) in buffer A in the rapid quench instrument (●). For analysis of the elemental effect on phosphodiester bond formation, T7$^-$ (32 nM, preincubated with 102 nM 25C/36G-mer) was mixed with a solution of dTTPαS (220 μM) in buffer A in the rapid quench instrument (□). All reactions were quenched by the addition of EDTA to 0.3 M. The burst equation $y = A(1 - e^{-k_p t}) + k_{ss}t$ was fit to the data, where A = burst amplitude, k_p = pre-steady-state rate constant for nucleotide incorporation, t = time, and k_{ss} = steady-state rate of nucleotide incorporation. The elemental effect was unity. (B) T7$^-$ (33 nM, preincubated with 102 nM 25C/36-8-oxoG-mer) was mixed with a solution of dTTP (220 μM) in buffer A in the rapid quench instrument (●). For analysis of the elemental effect on phosphodiester bond formation, T7$^-$ (30 nM, preincubated with 102 nM 25C/36-8-oxoG-mer) was mixed with a solution of dTTPαS (220 μM) in buffer A in the rapid quench instrument (□). The elemental effect was 2. (C) T7$^-$ (38 nM, preincubated with 102 nM 25A/36-8-oxoG-mer) was mixed with a solution of dTTP (220 μM) in buffer A in the rapid quench instrument (●). For analysis of the elemental effect on phosphodiester bond formation, T7$^-$ (37 nM, preincubated with 102 nM 25A/36-8-oxoG-mer) was mixed with a solution of dTTPαS (220 μM) in buffer A in the rapid quench instrument (□). The elemental effect was 5.

dTTPαS concentrations of 4, 6, and 9 mM (Supporting Information). The large thio effect strongly suggests that phosphodiester bond formation is rate-limiting for incorporation of dTTP following the Gua·A mispair.

Pre-Steady-State Kinetics of dTTP Incorporation Opposite 2-Aminopurine following Gua·C, 8-OxoGua·C, and 8-OxoGua·A Base Pairs. The low thio effects measured for incorporation of dTTP opposite A following Gua·C, 8-oxoGua·C, and 8-oxoGua·A base pairs suggest that conformational change is the rate-limiting step in each addition reaction. An additional model system was developed which could be used in both rapid-quench gel-based assays and in stopped-flow fluorescence quenching assays to better delineate contributions of conformational change and phosphodiester bond formation to the kinetic barrier for extension. In this case, 2-AP was substituted for A in the standing-start position of the template (Table 1). Although this substitution mimics the original model system and provides a mechanism by which to monitor the conformational change, it does not have the exact same kinetic profile as the model containing A (vide infra).

Pre-steady-state reactions were initiated by the rapid mixing of a preincubated solution of duplex DNA (102 nM, final) and T7$^-$ (37−44 nM, final) with dTTP in buffer A (Figure 4) as described above. As in the case of addition opposite A, incorporation of dTTP opposite 2-AP following Gua·C, 8-oxoGua·C, and 8-oxoGua·A base pairs showed biphasic kinetics with burst rates of ~75 s^{-1}, 1 s^{-1}, and 4 s^{-1}, respectively (Figure 4). When the normal dTTP was replaced by the thio analogue, dTTPαS (Figure 4), biphasic kinetics were eliminated for addition after both 8-oxoGua·C and 8-oxoGua·A base pairs. The Gua·C duplex still showed biphasic kinetics for incorporation of dTTPαS, but the burst rate was reduced to ~13 s^{-1}, a thio effect of ~6 (Figure 4A). The rates for dTTPαS addition after 8-oxoGua·C and 8-oxoGua·A base pairs were ~0.03 s^{-1} and ~0.2 s^{-1}, respectively, producing thio effects of ~30 and ~20, respectively (Figure 4B,C). These results suggest that the rate-limiting step during dTTP addition opposite 2-AP is phosphodiester bond formation, a different result than that observed for addition opposite A after 8-oxoGua·C and 8-oxoGua·A base pairs.

Stopped-Flow Fluorescence Quenching Assay of Incorporation of dTTP Opposite 2-Aminopurine. The presence of 2-AP in the standing start position of the template allowed the measurement of fluorescence quenching during incorporation of dTTP (Figure 5). Stopped-flow experiments contained 1.3 μM duplex DNA, 2.2 μM T7$^-$, and 200 μM dTTP (final concentrations). The dTTP concentration was saturating in each case.[3] Addition of dTTP opposite 2-AP following the Gua·C base pair fit a single-exponential rate equation very well, yielding a rate of 170 ± 20 s^{-1} (Figure 5A). Addition of dTTP opposite 2-AP following both 8-oxoGua·C and 8-oxoGua·A base pairs fit double-exponential plots but clearly not single-exponential plots. The

[3] The K_d for addition of dTTP opposite 2-AP after any of the three base pairs was determined to be <13 μM from rapid-quench experiments with varying concentrations of dTTP (Supporting Information).

[4] Attempts were made using dTTPαS substituted for dTTP, but definitive change in fluorescence was not detected due to signal drift.

[5] Additional stopped-flow experiments with the templates containing A in the standing start position were performed with dideoxy-terminated primers. In this case, the change in intrinsic protein fluorescence of T7$^-$ was measured over time (excitation at 295 nm, emission monitored with a 320 nm cutoff filter). Since T7$^-$ contains 18 tryptophan residues, we were hopeful that a fluorescence signal corresponding to protein conformational change would be observed. However, at 2 μM T7$^-$ and DNA and 200 μM dTTP, no change in fluorescence signal was detected. A confounding problem is the large excess of thioredoxin present in the polymerization system.

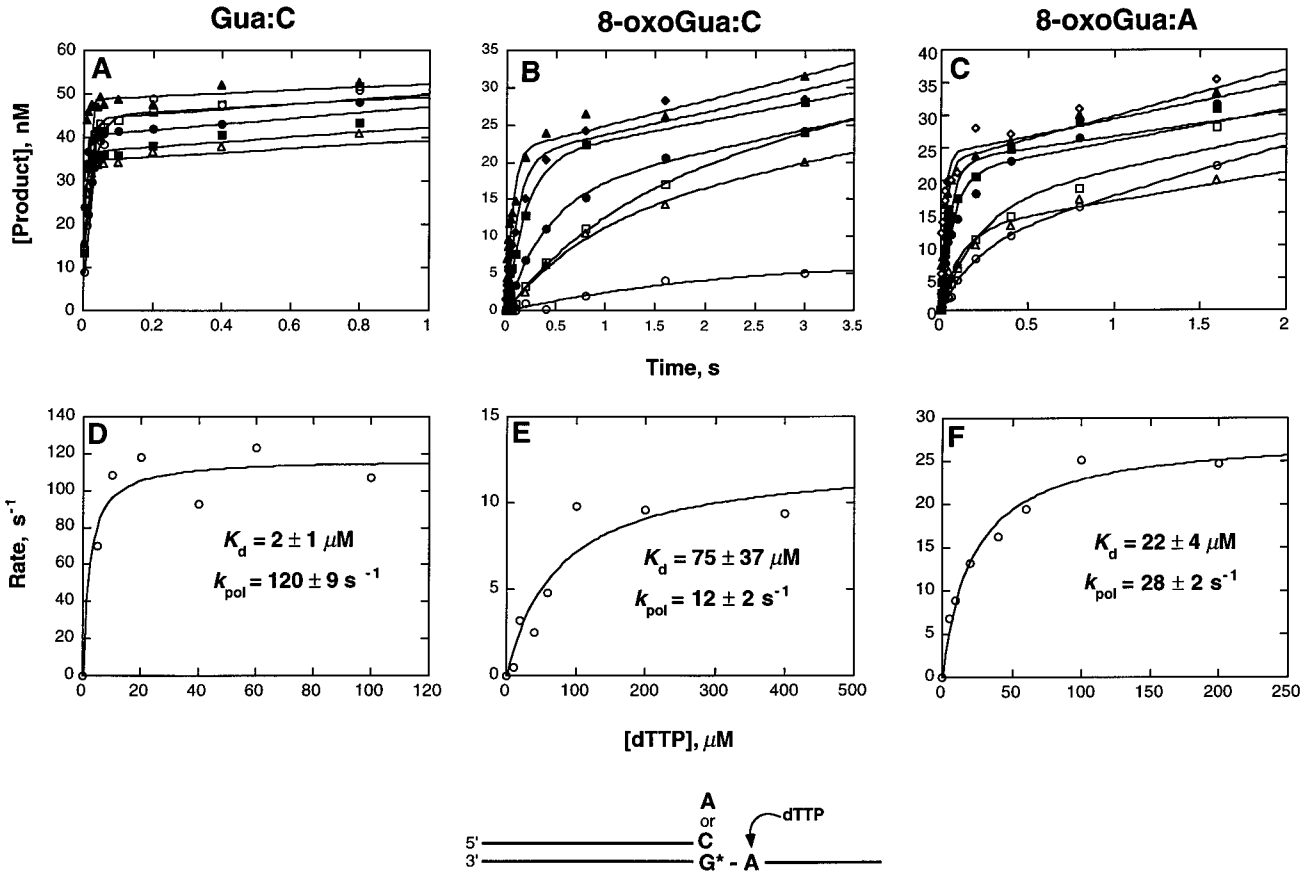

FIGURE 2: dTTP concentration dependence of the pre-steady-state burst rate for addition opposite A and determination of K_d and k_{pol}. (A) A preincubated solution of T7⁻ (25−38 nM) and 25C/36G-mer (102 nM) was mixed with increasing concentrations of dTTP (5.5 μM, ○; 11 μM, □; 22 μM, △; 44 μM, ●; 66 μM, ■; and 110 μM, ▲) in buffer A to start the reactions. The reactions were quenched over a time range of 0.005−3 s. (B) A preincubated solution of T7⁻ (22−34 nM) and 25C/36-8-oxoG-mer (102 nM) was mixed with increasing concentrations of dTTP (11 μM, ○; 22 μM, □; 44 μM, △; 66 μM, ●; 110 μM, ■; 220 μM, ▲; and 440 μM, ◆) in buffer A to start the reactions. The reactions were quenched over a time range of 0.005−3 s. (C) A preincubated solution of T7⁻ (24−32 nM) and 25A/36-8-oxoG-mer (102 nM) was mixed with increasing concentrations of dTTP (5.5 μM, ○; 11 μM, □; 22 μM, △; 44 μM, ●; 66 μM, ■; and 110 μM, ▲) in buffer A to start the reactions. The reactions were quenched over a time range of 0.005−3 s. The pre-steady-state rates of product formation in panels A, B, and C were determined by single-exponential analysis of the burst phase (see text for explanation) and then plotted against [dTTP] to determine K_d and k_{pol} for incorporation of dTTP by T7⁻ following (D) Gua·C base pair, (E) 8-oxoGua·C base pair, or (F) 8-oxoGua·A base pair.

Table 2: Kinetic Parameters for T7⁻ Next Correct Base Addition Opposite A

	steady-state			pre-steady-state		
	K_m (μM)	k_{cat} (s^{-1})	k_{cat}/K_m (s^{-1} μM^{-1})[a]	K_d (μM)	k_{pol} (s^{-1})	k_{pol}/K_d (s^{-1} μM^{-1})[a]
Gua·C	0.24 ± 0.05	0.34 ± 0.02	1.4	2 ± 1	120 ± 9	60
Gua·A	1700 ± 500	0.011 ± 0.002	6.5×10^{-6}	ND[b]	−[c]	ND[b]
8-oxoGua·C	22 ± 3	0.17 ± 0.01	7.7×10^{-3}	75 ± 37	12 ± 2	0.2
8-oxoGua·A	0.7 ± 0.2	0.046 ± 0.007	7×10^{-2}	22 ± 4	28 ± 2	1.3

[a] Efficiency of extension. [b] ND, not determined. [c] From single-turnover experiments using 2 mM (final) dTTP, a rate of 6.7×10^{-3} s^{-1} was obtained (see Figure 3 and text for details).

initial and second-exponential rates for addition following 8-oxoGua·C were 3 ± 1 s^{-1} and 0.55 ± 0.01 s^{-1} (Figure 5B). For addition following 8-oxoGua·A, the rates were 37 ± 8 s^{-1} and 1.94 ± 0.02 s^{-1} (Figure 5C).[4,5]

DISCUSSION

The preferential extension of DNA adduct mismatches versus extension of the adduct paired with the correct base presents a mechanism by which replication errors leading to mutagenesis can be propagated by polymerases. One explanation for the preferential extension of adduct mismatches that has been offered is that the polymerase binds the adduct mismatch duplex DNA preferentially over duplex DNA containing the adduct with the correct base. However, a large number of groups working with a variety of DNA adduct pairs [including 8-oxoGua pairs (*14*, *15*)] and a variety of DNA polymerases have shown that polymerases bind mismatched termini efficiently (*3*, *7*, *14*, *15*, *22*−*24*). The preferential extension of the mismatch or the replication blocking potential of an adduct correct pair is, then, believed to be controlled by a kinetic barrier to extension.

We and others have examined the pre-steady-state kinetics of extension of adduct mismatches. Tan et al. (*25*) showed that an O^6-methylGua·T pair was extended more efficiently

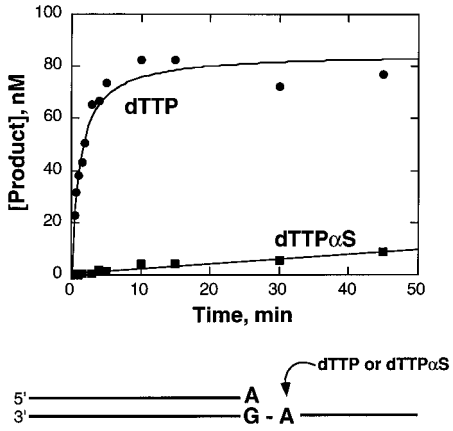

FIGURE 3: Single-turnover elemental effect for dTTP incorporation opposite A following a Gua·A mispair. Reactions were initiated by the manual addition of dTTP (●) or dTTPαS (■) (2 mM, final) to T7$^-$ (70 nM, final) preincubated with 25A/36G-mer (100 nM, final) followed by quenching with 20 mM EDTA at the indicated times. The time course for addition of dTTP (●) was 6.7×10^{-3} s^{-1} and of dTTPαS (■) was 4.6×10^{-5} s^{-1}, yielding an elemental effect of 150.

than O^6-methylGua·C, but the kinetic parameters governing those results were not defined. In previous work with KF$^-$, pol II$^-$, HIV-1 RT, and T7$^-$, we showed in rapid-quench assays that 8-oxoGua·A base pairs were extended more efficiently than 8-oxoGua·C in all cases (*14*, *15*), but only now have we attempted to clearly define what the kinetic and mechanistic basis for these results are using T7$^-$ as our model polymerase.

The burst analyses done previously with T7$^-$ (*15*) were repeated presently with the new template containing A in the standing start position, and again we found biphasic kinetics for addition of the next correct base following Gua·C, 8-oxoGua·C, and 8-oxoGua·A base pairs, suggesting that phosphodiester bond formation or a step before phosphodiester bond formation is rate-limiting in the single-turnover mechanism. The modest thio effects (from 1 to 6) observed in the elemental effect experiments suggest that the conformational change prior to phosphodiester bond formation is the rate-limiting step in the mechanism of correct base addition following Gua·C, 8-oxoGua·C, and 8-oxoGua·A base pairs. Thus, mechanistically, all three extension reactions above appear to be governed by the same rate-limiting step. The thio effect of ~150 for nucleotide addition following a Gua·A base pair strongly suggests that phosphodiester bond formation is the rate-limiting step for that extension reaction in agreement with previous analysis of nucleotide addition by T7$^-$ following a mispair (*3*).

Differences in the pre-steady-state parameters K_d (dNTP dissociation constant) and k_{pol} (the maximum rate for nucleotide incorporation) for addition of dTTP opposite A following Gua·C, 8-oxoGua·C, and 8-oxoGua·A base pairs help to define the kinetic barrier to extension of 8-oxoGua·C and the preferential extension of 8-oxoGua·A. Extension of a normal base pair, Gua·C, proceeds more readily than extension of either 8-oxoGua base pair, with a k_{pol} of 120 ± 9 s^{-1}, a K_d of 2 ± 1 μM, and an overall efficiency (k_{pol}/K_d) of ~60 s^{-1} μM^{-1}. The k_{pol} for extension of 8-oxoGua·A was 2-fold greater than the k_{pol} for extension of 8-oxoGua·C (28 ± 2 s^{-1} vs 12 ± 2 s^{-1}), and additionally the K_d for extension of 8-oxoGua·A was one-third the K_d for extension of 8-oxoGua·C (22 ± 4 μM vs 75 ± 37 μM). These results suggest that the preferential extension of 8-oxoGua·A is due to a larger rate constant for nucleotide addition and lower K_d^{dTTP}. The combined effects of higher k_{pol} and lower K_d for extension of 8-oxoGua·A yield an efficiency of extension ~7-fold greater than that for extension of 8-oxoGua·C (1.3 s^{-1} μM^{-1} vs 0.2 s^{-1} μM^{-1}). From previous work with T7$^-$ (*15*), the efficiencies (k_{pol}/K_d) for *forming* Gua·C, 8-oxoGua·C, and 8-oxoGua·A base pairs were approximately 27 s^{-1} μM^{-1}, 0.2 s^{-1} μM^{-1}, and 0.002 s^{-1} μM^{-1}, respectively, in this oligonucleotide pair.

To define more rigorously the contributions of phosphodiester bond formation and the conformational change before phosphodiester bond formation to the kinetic barrier for adduct base pair extension, an additional model system was used in which the template A was replaced with a fluorescent base analogue, 2-AP. This model system has been used previously to provide direct evidence for the conformational change prior to phosphodiester bond formation in the mechanisms of bacteriophage T4 DNA polymerase and KF (*26*). In our experiments, the 2-AP is at the standing start position of the template, and the 3′-termini of the duplex contains either a Gua·C, 8-oxoGua·C, or 8-oxoGua·A base pair. Initial rapid-quench burst assays showed a biphasic response for addition of dTTP opposite 2-AP following each of the three base pairs, suggesting that phosphodiester bond formation or a step before is rate-limiting. Substitution of dTTP with the thio analogue, dTTPαS, resulted in a loss of biphasic kinetics during addition following both 8-oxoGua pairs but not for addition following Gua·C. The thio effects of 30 and 20 observed for addition after 8-oxoGua·C and 8-oxoGua·A, respectively, strongly suggests that phosphodiester bond formation is the rate-limiting step in the mechanism of extension.

The results of stopped-flow fluorescence quenching assays with the 2-AP-containing template supported and expanded the rapid-quench results. Addition of dTTP following Gua·C showed a single-exponential trace with a rate ~2-fold the burst rate determined from rapid-quench assays. The kinetic traces for nucleotide addition following both of the 8-oxoGua base pairs fit a double exponential with an initial fast rate followed by a slower second rate, which was nearly the same as the burst rate determined from rapid-quench experiments with each 8-oxoGua base pair. The initial rates in the traces for nucleotide addition following 8-oxoGua·C and 8-oxoGua·A occurred at rates of 3 ± 1 s^{-1} and 37 ± 8 s^{-1}, respectively. The initial rate of fluorescence quenching measured is faster than product formation in rapid-quench gel based assays and thus is postulated to reflect the rate of the conformational change prior to phosphodiester bond formation (it is probably too slow to be dNTP binding). In this case, there is a larger difference between the rates of conformational change than between phosphodiester bond formation rates in extension of 8-oxoGua·C and 8-oxoGua·A base pairs. Thus, the kinetic and mechanistic barrier to extension of the 8-oxoGua·C base pair may reside in discrimination at the conformational change level, although overall discrimination in extension of either 8-oxoGua base pair compared to the Gua·C base pair is at the level of phosphodiester bond formation when 2-AP is in the standing start position since both 8-oxoGua base pairs show a phosphodiester bond formation rate-limiting step.

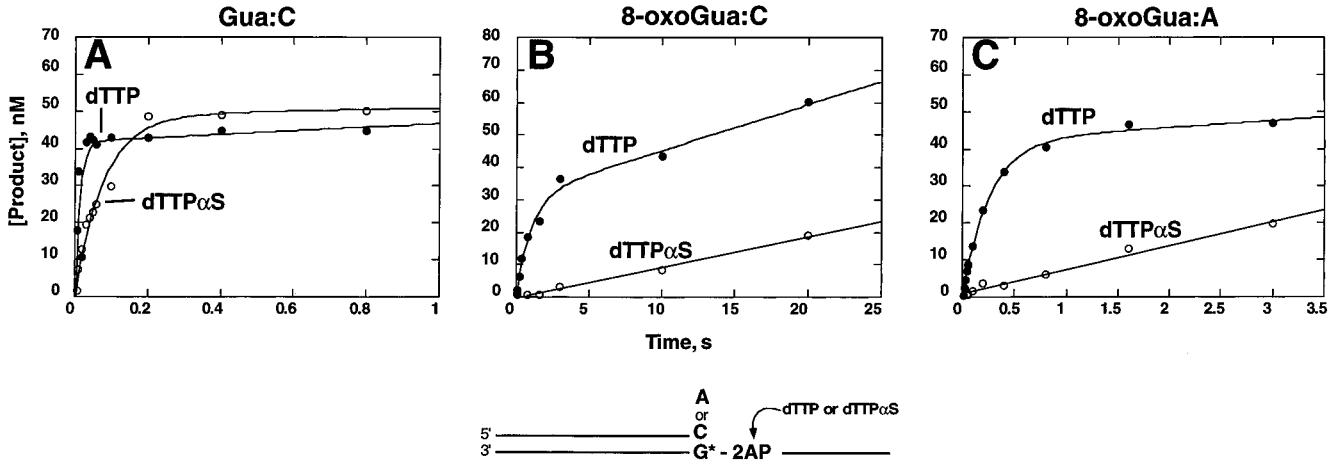

FIGURE 4: Time progress and elemental effect for dTTP incorporation opposite 2-AP following Gua·C, 8-oxoGua·C, and 8-oxoGua·A base pairs. (A) T7⁻ (37 nM, preincubated with 102 nM 25C/36G-2AP-mer) was mixed with a solution of dTTP (220 μM) in buffer A in the rapid quench instrument (●). For analysis of the elemental effect on phosphodiester bond formation, T7⁻ (37 nM, preincubated with 102 nM 25C/36G-2AP-mer) was mixed with a solution of dTTPαS (220 μM) in buffer A in the rapid quench instrument (□). The elemental effect was 6. All reactions were quenched by the addition of EDTA to 0.3 M. The burst equation $y = A(1 - e^{-k_p t}) + k_{ss}t$ was fit to the data, where A = burst amplitude, k_p = pre-steady-state rate for nucleotide incorporation, t = time, and k_{ss} = steady-state rate of nucleotide incorporation. (B) T7⁻ (44 nM, preincubated with 102 nM 25C/36-8-oxoG-2AP-mer) was mixed with a solution of dTTP (220 μM) in buffer A in the rapid quench instrument (●). For analysis of the elemental effect on phosphodiester bond formation, T7⁻ (38 nM, preincubated with 102 nM 25C/36-8-oxoG-2AP-mer) was mixed with a solution of dTTPαS (220 μM) in Buffer A in the rapid quench instrument (□). The elemental effect was 32. (C) T7⁻ (41 nM, preincubated with 102 nM 25A/36-8-oxoG-2AP-mer) was mixed with a solution of dTTP (220 μM) in buffer A in the rapid quench instrument (●). For analysis of the elemental effect on phosphodiester bond formation, T7⁻ (41 nM, preincubated with 102 nM 25A/36-8-oxoG-2AP-mer) was mixed with a solution of dTTPαS (220 μM) in buffer A in the rapid quench instrument (□). The elemental effect was 24.

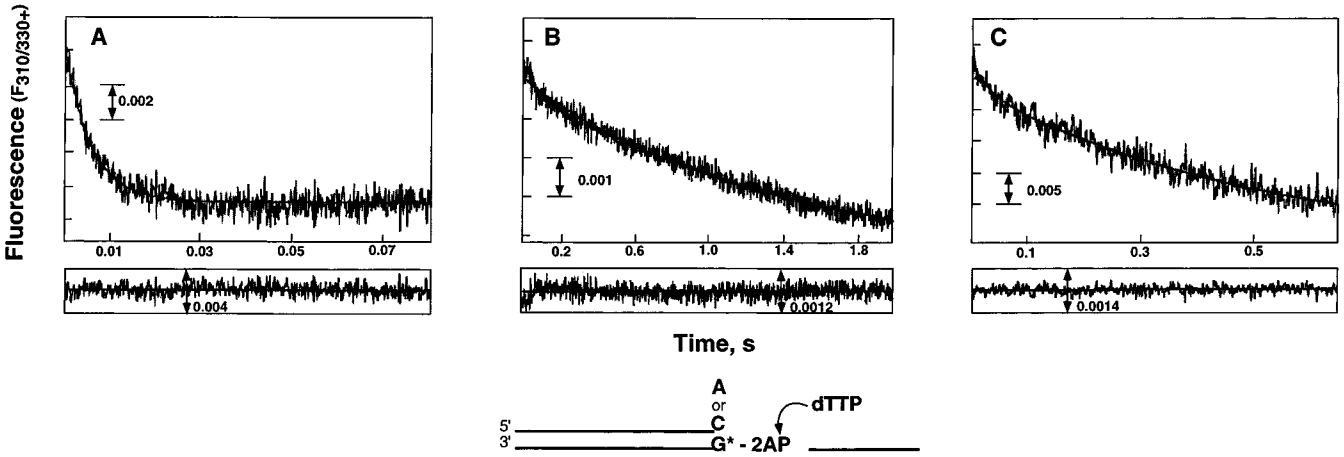

FIGURE 5: Stopped-flow fluorescence quenching assay of incorporation of dTTP opposite 2-aminopurine. (A) Extension of the Gua·C base pair. Excess T7⁻ (2.2 μM) preincubated with duplex DNA with 2-AP in the standing start position (1.3 μM) was rapidly mixed with an equal volume of 200 μM dTTP at 25 °C. The data shown are an average of four consecutive runs fit to a single exponential. The rate constant was determined to be 170 ± 20 s^{-1}. (B) Extension of the 8-oxoGua·C base pair. Experiments were performed as described above. The data shown are an average of five consecutive runs fit to a double-exponential function. The initial and second rate constants were determined to be 3 ± 1 s^{-1} and 0.55 ± 0.01 s^{-1}, respectively. (C) Extension of the 8-oxoGua·A base pair. Experiments were performed as described above. The data shown are an average of 10 consecutive runs fit to a double-exponential function. The initial and second rate constants were determined to be 37 ± 8 s^{-1} and 1.94 ± 0.02 s^{-1}, respectively. Residual analysis is shown below each of the traces, as described under Experimental Procedures.

In conclusion, with A in the standing start position following Gua·C, 8-oxoGua·C, and 8-oxoGua·A base pairs, the rate-limiting step in the mechanism of T7⁻ appears to be the conformational change before phosphodiester bond formation with all three base pairs. Thus, the adduct-containing pairs do not appear to alter the general mechanism of T7⁻. The kinetic barrier to extension of the 8-oxoGua·C base pair is best described by the smaller k_{pol} and larger K_d values compared to those for extension of 8-oxoGua·A. Furthermore, extrapolating from stopped-flow fluorescence quenching experiments with 2-AP in the standing start position, the conformational change prior to phosphodiester bond formation may be the more discriminatory step in preferential extension of 8-oxoGua·A based on the differences in conformational change rates compared to the smaller differences in phosphodiester bond formation rates.

SUPPORTING INFORMATION AVAILABLE

Elemental effect studies with Gua·A mismatch and 4, 6, and 9 mM dTTP and dTTPαS and determination of K_d and k_{pol} for addition of dTTP opposite 2-AP (4 pages). Ordering information is given on any current masthead page.

REFERENCES

1. Kuchta, R. D., Benkovic, P., and Benkovic, S. J. (1988) *Biochemistry 27*, 6716−6725.
2. Eger, B. T., and Benkovic, S. J. (1992) *Biochemistry 31*, 9227−9236.
3. Wong, I., Patel, S. S., and Johnson, K. A. (1991) *Biochemistry 30*, 526−537.
4. Petruska, J., Goodman, M. F., Boosalis, M. S., Sowers, L. C., Cheong, C., and Tinoco, I., Jr. (1988) *Proc. Natl. Acad. Sci. U.S.A. 85*, 6252−6256.
5. Goodman, M. F., Creighton, S., Bloom, L. B., and Petruska, J. (1993) *Crit. Rev. Biochem. Mol. Biol. 28*, 83−126.
6. Larroque, C., Lange, R., Maurin, L., Bienvenue, A., and van Lier, J. E. (1990) *Arch. Biochem. Biophys. 282*, 198−201.
7. Creighton, S., Huang, M. M., Cai, H., Arnheim, N., and Goodman, M. F. (1992) *J. Biol. Chem. 267*, 2633−2639.
8. Zinnen, S., Hsieh, J. C., and Modrich, P. (1994) *J. Biol. Chem. 269*, 24195−24202.
9. Dosanjh, M. K., Galeros, G., Goodman, M. F., and Singer, B. (1991) *Biochemistry 30*, 15595−11599.
10. Dosanjh, M. K., Menichini, P., Eritja, R., and Singer, B. (1993) *Carcinogenesis 14*, 1915−1919.
11. Hanrahan, C. J., Bacolod, M. D., Vyas, R. R., Liu, T., Geacintov, N. E., Loechler, E. L., and Basu, A. K. (1997) *Chem. Res. Toxicol. 10*, 369−377.
12. Hashim, M., and Marnett, L. J. (1996) *J. Biol. Chem. 271*, 9160−9165.
13. Shibutani, S., Takeshita, M., and Grollman, A. P. (1991) *Nature 349*, 431−434.
14. Lowe, L. G., and Guengerich, F. P. (1996) *Biochemistry 35*, 9840−9849.
15. Furge, L. L., and Guengerich, F. P. (1997) *Biochemistry 36*, 6475−6487.
16. Laemmli, U. K. (1970) *Nature 227*, 680−685.
17. Kati, W. M., Johnson, K. A., Jerva, L. F., and Anderson, K. S. (1991) *Biochemistry 30*, 511−525.
18. Lunn, C. A., Kathju, S., Wallace, B. J., Kushner, S. R., and Pigiet, V. (1984) *J. Biol. Chem. 259*, 10469−10474.
19. Borer, P. N. (1975) in *Handbook of Biochemistry and Molecular Biology, 3rd ed* (Fasman, G. D., Ed.) pp 589−580, CRC Press, Cleveland, OH.
20. Boosalis, M. S., Petruska, J., and Goodman, M. F. (1987) *J. Biol. Chem. 262*, 14689−14696.
21. Johnson, K. A. (1995) *Methods Enzymol. 249*, 38−61.
22. Mendelman, L. V., Petruska, J., and Goodman, M. F. (1990) *J. Biol. Chem. 265*, 2338−2346.
23. Yu, H., and Goodman, M. F. (1992) *J. Biol. Chem. 267*, 10888−10896.
24. Huang, M. M., Arnheim, N., and Goodman, M. F. (1992) *Nucleic Acids Res. 20*, 4567−4573.
25. Tan, H. B., Swann, P. F., and Chance, E. M. (1994) *Biochemistry 33*, 5335−5346.
26. Frey, M. W., Sowers, L. C., Millar, D. P., and Benkovic, S. J. (1995) *Biochemistry 34*, 9185−9192.

BI9722094